



PAPER

A SINS/GNSS/2D-LDV integrated navigation scheme for unmanned ground vehicles

To cite this article: Zhiyi Xiang *et al* 2023 *Meas. Sci. Technol.* **34** 125116

View the [article online](#) for updates and enhancements.

You may also like

- [Experimental research on flow field in the draft tube of pump turbines based on LDV](#)
D M Liu, Y Z Zhao and Z G Zuo
- [An Improved Method Using SINS/PPP Method for Land Vehicle Gravimetry](#)
R H Yu, L Wang, J L Cao et al.
- [An adaptive Kalman filtering algorithm based on maximum likelihood estimation](#)
Zili Wang, Jianhua Cheng, Bing Qi et al.

A SINS/GNSS/2D-LDV integrated navigation scheme for unmanned ground vehicles

Zhiyi Xiang^{1,2} , Tao Zhang^{1,2}, Qi Wang^{1,2}, Shilong Jin^{1,2}, Xiaoming Nie^{1,2}, Chengfang Duan^{1,2} and Jian Zhou^{1,2,*} 

¹ College of Advanced Interdisciplinary Studies, National University of Defense Technology, Changsha 410073, People's Republic of China

² Nanhu Laser Laboratory, National University of Defense Technology, Changsha 410073, People's Republic of China

E-mail: wttzhoujian@163.com

Received 27 June 2023, revised 25 July 2023

Accepted for publication 22 August 2023

Published 30 August 2023



Abstract

In recent years, unmanned autonomous driving technology has attracted increasing attention from people, and become a research hotspot. Currently, the integration of strapdown inertial navigation system (SINS) and global navigation satellite systems (GNSSs) is the most common and effective navigation and positioning scheme for unmanned ground vehicles (UGVs) and unmanned aerial vehicles. However, this integrated system is unable to maintain a reliable positioning solution in challenging environments due to the inherent weakness of GNSS signals and the accumulation of SINS positioning errors over time. To address this issue, this paper proposes an integrated scheme based on an asynchronous Kalman filter for SINS, GNSS and two-dimensional (2D) laser Doppler velocimeter (LDV). In the proposed scheme, the SINS and 2D-LDV are tightly coupled to improve the robustness of the integrated system, and the error parameters between the 2D-LDV and the SINS are calibrated in real time during the validity of the GNSS signal. In addition, the designed asynchronous Kalman filter method evaluates the validity of the GNSS and 2D-LDV measurements in real time based on Mahalanobis distance of innovation vector and statistical property principle. Two groups of long-distance, high-mobility vehicle experiments conducted in challenging environments verify the validity of the proposed scheme. The experimental results show that the proposed SINS/GNSS/2D-LDV integrated navigation scheme has good environmental adaptability and reliability, and can maintain high horizontal and vertical positioning accuracy despite frequent GNSS signal failures, which can meet the needs of UGVs.

Keywords: strapdown inertial navigation system (SINS), laser Doppler velocimeter (LDV), SINS/GNSS/2D-LDV integrated navigation scheme

(Some figures may appear in colour only in the online journal)

1. Introduction

Unmanned autonomous driving technology has attracted considerable attention from both academia and industry in recent

years. Consequently, the need for reliable, continuous and high-precision navigation technology has become more urgent than ever. Strapdown inertial navigation system (SINS) is an autonomous navigation system that has the advantages of strong anti-jamming capability, high sampling rate, and good concealment [1]. However, as a dead reckoning system, SINS's positioning errors accumulate over time [2, 3]. Global

* Author to whom any correspondence should be addressed.

navigation satellite system (GNSS) can provide highly accurate position and velocity information for unmanned ground vehicles (UGVs) on a global scale, which is crucial for their operation. Nevertheless, GNSS has poor dynamic performance, poor anti-interference capability, and signals that are easily blocked by tall trees and buildings [4]. These defects of GNSS can often lead to fatal consequences for UGV in practical applications. Since SINS and GNSS have complementary strengths, their integration is an effective way to achieve high-quality and high-stability navigation for land vehicles [5].

Although SINS/GNSS is the most common navigation mode for land vehicle navigation systems, it has some limitations in complex and harsh urban environments. In these environments, GNSS signals can be blocked by buildings, bridges and trees, or affected by multipath effects in canyons and tunnels [6–10]. As a result, GNSS may not be able to output valid navigation information, and the positioning accuracy of the SINS/GNSS integrated navigation system may not meet the specific requirements of UGV. Furthermore, when GNSS is denied for a long time, the SINS/GNSS integrated navigation system will degenerate into a pure inertial navigation system and navigation errors will diverge rapidly over time. Unlike GNSS, odometer (OD), laser Doppler velocimeter (LDV), camera, and LIDAR are fully autonomous sensors whose measurements are less affected by external interference and whose measurement errors do not accumulate over time. Therefore, in GNSS-denied environments, the introduction of OD, LDV, camera and LIDAR sensors can help suppress the divergence of UGV navigation errors [11–14].

Since OD does not rely on external signals, the SINS/OD integration is one of the most common land autonomous navigation modes in GNSS-denied scenarios [15–21]. OD is typically mounted on the tire of the vehicle and measures the angle of wheel rotation. By combining this with the circumference of the wheel and the travel time of the vehicle, the velocity and distance travelled of the vehicle can be obtained. However, the accuracy of OD is closely related to the travel state of the vehicle and the condition of the wheel. Factors such as wheel temperature, air pressure, wear and tear, and jumping and slipping during vehicle movement will reduce the accuracy of OD measurement. Camera and lidar can provide continuous position, attitude, and environment information to vehicles and are widely used in autonomous driving, but they still face some practical challenges, such as high computational costs, and unreliability in harsh environments and high-speed movements.

LDV is a laser scattering-based instrument that uses the Doppler shift of scattered light from moving particles to determine the velocity of the particles. It is a fully autonomous velocity sensor with the advantages of high measurement accuracy, non-contact measurement, good spatial resolution, fast dynamic response, wide range of velocity measurement, and high directional sensitivity [22]. Compared to the OD, the advantage of non-contact measurement makes the output of the LDV independent of the state of the vehicle tire, so LDV has excellent scale factor stability and higher measurement accuracy, which helps to improve the horizontal positioning

accuracy of the combined navigation system. In recent years, LDVs have been used on a small scale in the domain of terrestrial navigation autonomously [23–30].

In conclusion, the integration of SINS, GNSS and LDV is undoubtedly extremely suitable for UGV. The addition of LDV can enable UGV to maintain high navigation accuracy even when GNSS fails for a short or long time. Furthermore, the SINS/GNSS/LDV integration is likely to be more reliable than the traditional SINS/GNSS/OD integration in most cases because of the excellent performance of LDV. In a recent study, Du *et al* proposed an SINS/GNSS/LDV tightly coupled seamless navigation technique, and demonstrated its effectiveness and reliability [14]. However, what is used in this method is one-dimensional LDV (1D-LDV), which, like OD, can only provide the forward velocity of the vehicle, but not the upward velocity of the vehicle, and its three-dimensional (3D) velocity information is obtained by combining the well-known non-holonomic constraints (NHC) assumptions, which will not be able to constrain the upward error of the vehicle when the vehicle has large upward maneuvering during the period of GNSS failure effectively. In addition, the method only uses a conventional centralized Kalman filter to fuse the information from the three sensors, and the conventional centralized Kalman filter has the following two main shortcomings: firstly, the conventional centralized Kalman filter cannot identify and isolate the abnormal information of the sensor in the navigation process, which will make the abnormal value of the sensor contaminate the integrated navigation result; and secondly, the conventional centralized Kalman filter cannot process the information of sensors with different frequencies well, which will inevitably lead to the waste of effective information of sensors. The above shortcomings in the literature [14] also exist in the existing SINS/GNSS/OD integrated navigation methods.

To address the above shortcomings, this paper proposes a high-precision integrated navigation method that uses two-dimensional LDV (2D-LDV) to assist SINS and GNSS, and aims to realize high-precision positioning of UGV in the GNSS-denied environment. Unlike 1D-LDV and OD, 2D-LDV can provide both the forward and the upward velocity of the vehicle, and the precise upward velocity of the vehicle can effectively inhibit the divergence of SINS height errors when GNSS fails. In addition, in the proposed method, the SINS/2D-LDV tightly coupled model is used to enhance the robustness of the system, and the error parameters of the SINS/2D-LDV tightly coupled model are calibrated in real time during the validity of the GNSS signals to improve the performance of the system. For the processing of sensor information from multiple sensors of different frequencies, an asynchronous Kalman filter is designed in this paper, and sensor outliers are detected and isolated in time. Vehicle-mounted experiments are conducted to validate the effectiveness of the proposed method. Comparing with previous works, the contributions of this paper include:

- (1) Unlike previous methods that used OD, 1D-LDV and vehicle dynamics model (VDM) to assist SINS and GNSS,

this is the first time that 2D-LDV is used to assist SINS and GNSS. The forward velocity and upward velocity provided by 2D-LDV can ensure that when GNSS cannot provide high-quality and effective navigation information, the UGV can still achieve satisfactory horizontal and height positioning accuracy.

- (2) According to the characteristics of the optical path structure of the 2D-LDV laser, a more robust SINS/2D-LDV tightly coupled model based on the velocity information under the LDV beam frame obtained from each beam of 2D-LDV is established to improve the reliability of the SINS/2D-LDV integrated navigation system when GNSS fails.
- (3) The included angle between the two beams of the 2D-LDV and the misalignment angles between the body frame and the LDV frame are calibrated in real time using GNSS when GNSS signals are good to reduce the influence of the changes in the structural rigidity of the vehicle and in the characteristics of the laser inside the LDV on the accuracy of the system during the travel of the vehicle.
- (4) An asynchronous Kalman filter is designed based on the idea of sequential Kalman filter to fuse three different frequency sensors—SINS, GNSS and 2D-LDV—to make full use of all available observations, and the outliers of GNSS and 2D-LDV are detected based on Mahalanobis distance and statistical property principle.
- (5) Considering that the current work related to SINS/GNSS/OD and SINS/GNSS/VDM is carried out in urban areas and most of them are short-range experiments, two groups of long-distance high-mobility land vehicle tests are carried out, which involve different driving environments (open-sky, urban canyons, tunnels, viaducts, boulevards, etc). The high-precision IMU is used for reference and the medium-precision IMU is used for system testing. The effectiveness of the technique proposed in this paper is evaluated by comparing it with SINS/GNSS/1D-LDV and SINS/GNSS.

The rest of this paper is organized as follows. In section 2, the SINS/GNSS/1D-LDV integrated navigation method is introduced. In section 3, an SINS/GNSS/2D-LDV integrated navigation scheme based on an asynchronous Kalman filter is proposed. In section 4, the proposed integrated navigation scheme is compared with the SINS/GNSS/1D-LDV and SINS/GNSS by using the vehicle-mounted field test data collected from the SINS/GNSS/2D-LDV integrated navigation system. Concluding remarks are given in section 5.

2. Review of SINS/GNSS/1D-LDV system

The installation relationship between the LDV, IMU and GNSS is shown in figure 1. The LDV body frame, denoted by m frame, is defined as right-forward-upward. The IMU body frame, denoted by b frame, is also defined as right-forward-upward. The navigation frame is defined as east-north-up and is denoted by the n frame.

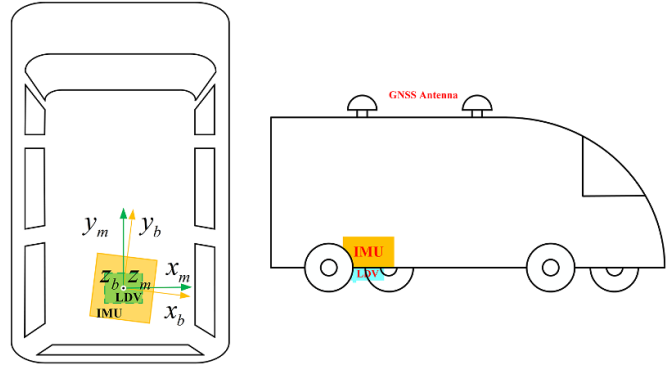


Figure 1. Installation relationship between the LDV, IMU and GNSS.

2.1. SINS model

The SINS calculates the navigation parameters of the vehicle based on the outputs of gyroscopes and accelerometers. In the n frame, the SINS error equations and the estimated parameters of SINS can be expressed as [31]:

$$\begin{cases} \dot{\varphi} = \varphi \times \omega_{in}^n + \delta\omega_{in}^n - C_b^n \epsilon_{ib}^b \\ \delta\dot{v}_{SINS}^n = -\varphi \times f^n + \delta v_{SINS}^n \times (2\omega_{ie}^n + \omega_{en}^n) \\ \quad + v_{SINS}^n \times (2\delta\omega_{ie}^n + \delta\omega_{en}^n) + C_b^n \nabla_{ib}^b \\ \delta\dot{L} = \delta v_N / (R_M + h) - v_N \delta h / (R_M + h)^2 \\ \delta\dot{\lambda} = \sec L \delta v_E / (R_N + h) + v_E \tan L \sec L \delta L / (R_N + h) \\ \quad - v_E \sec L \delta h v_E / (R_N + h)^2 \\ \delta\dot{h} = \delta v_U \\ \dot{\epsilon}_{ib}^b = \mathbf{0}_{3 \times 1} \\ \dot{\nabla}_{ib}^b = \mathbf{0}_{3 \times 1} \end{cases} \quad (1)$$

$$X_{SINS} = \begin{bmatrix} \varphi^T & \delta(v_{SINS}^n)^T & \delta p_{SINS}^T & (\epsilon_{ib}^b)^T & (\nabla_{ib}^b)^T \end{bmatrix}^T \quad (2)$$

where φ denote the attitude error of SINS, C_b^n is the transformation matrix from b frame to n frame; $(\cdot) \times$ means to solve the antisymmetric matrix, $\mathbf{0}_{3 \times 1}$ denotes the 3×1 zero vector; $v_{SINS}^n = [v_E \ v_N \ v_U]^T$ is the velocity of SINS, and $\delta v_{SINS}^n = [\delta v_E \ \delta v_N \ \delta v_U]^T$ is the velocity error of the SINS; R_M and R_N are the principal radius of curvature of the prime meridian and the equator, respectively; $\delta p_{SINS} = [\delta L \ \delta \lambda \ \delta h]^T$ denotes position error vectors of SINS; L , λ , and h are the local latitude, local longitude, and local altitude, respectively; ω_{in}^n , ω_{en}^n , and ω_{ie}^n are the rotation angular rate vectors of the n frame relative to the inertial frame, the n frame relative to the earth frame, and the earth frame relative to the inertial frame, respectively, and all vectors are projected in the n frame; f^n denotes the specific force output from accelerometers in the n frame; ϵ_{ib}^b and ∇_{ib}^b are the gyro constant bias and the accelerometer constant bias, respectively.

2.2. SINS/1D-LDV model

In the SINS/1D-LDV integrated navigation system, 1D-LDV only provides the 1D velocity along the vehicle trajectory and uses the NHC of land vehicles to achieve 3D velocity measurements. Therefore, the vehicle velocity measured by the 1D-LDV in the m frame can be expressed as

$$\mathbf{v}_{LDV}^m = [0 \quad v_{LDV} \quad 0]^T \quad (3)$$

where v_{LDV} denotes the output of the 1D-LDV and is given by

$$v_{LDV} = \lambda f_D / (2 \cos \beta) = K f_D \quad (4)$$

where λ is the wavelength of the laser, f_D is the Doppler frequency, β is the inclination angle of the laser beam incident on the ground, and K is the scale factor of LDV.

As (4) shows, the scale factor of the 1D-LDV is related to the wavelength of the laser and the inclination angle of 1D-LDV design. However, due to the deviation between the actual and designed inclination of the 1D-LDV and between the actual and designed wavelength of the laser, there is a scale factor error between the output velocity of the 1D-LDV and the true velocity. Therefore, (3) can be rewritten as

$$\mathbf{v}_{LDV}^m = (1 + \delta K) \mathbf{v}^m \quad (5)$$

where \mathbf{v}^m is the true velocity of the vehicle in the m frame when the NHC condition is satisfied.

In general, the misalignment angles between the b frame and the m frame are inevitable due to installation conditions, but can be easily controlled to a sufficiently small level. Moreover, it is usually calibrated beforehand in order to improve the accuracy of the SINS/1D-LDV integrated navigation. Thus, the velocity of 1D-LDV in the b frame can be expressed as

$$\mathbf{v}_{LDV}^b = (\mathbf{I}_3 - \phi_m \times) \mathbf{C}_m^b (1 + \delta K) \mathbf{v}^m \quad (6)$$

where \mathbf{I}_3 is the 3×3 identity matrix, \mathbf{C}_m^b is the transformation matrix from the m frame to the b frame, and ϕ_m denotes the error of the misalignment angles between the m frame and the b frame after calibration defined as

$$\phi_m = [\phi_{mx} \quad \phi_{my} \quad \phi_{mz}]^T \quad (7)$$

where ϕ_{mx} , ϕ_{my} , and ϕ_{mz} denote the errors of pitch, roll and heading misalignment angles between the m frame and the b frame, respectively.

Note that the effect of the lever arm is not considered here because the LDV and IMU are mounted vertically and close to each other in this paper.

Based on (6), the velocity of 1D-LDV in the n frame is as follows

$$\mathbf{v}_{LDV}^n = (\mathbf{I}_3 - \varphi \times) \mathbf{C}_b^n (\mathbf{I}_3 - \phi_m \times) \mathbf{C}_m^b (1 + \delta K) \mathbf{v}^m \quad (8)$$

where \mathbf{C}_b^n is the attitude matrix from the b frame to the n frame.

To summarize, for the SINS/1D-LDV integrated navigation model, the velocity observation can be written as:

$$\begin{aligned} \mathbf{v}_{LDV}^n - \mathbf{v}_{SINS}^n &= (\mathbf{I}_3 - \varphi \times) \mathbf{C}_b^n (\mathbf{I}_3 - \phi_m \times) (1 + \delta K) \mathbf{v}^m \\ &\quad - \mathbf{v}^n - \delta \mathbf{v}_{SINS}^n \\ &\approx (\mathbf{v}^n \times) \varphi + \mathbf{C}_b^n (\mathbf{v}^m \times) \phi_m + \mathbf{v}^n \delta K - \delta \mathbf{v}_{SINS}^n \end{aligned} \quad (9)$$

where \mathbf{v}^n denotes the vehicle true velocity in the n frame.

As can be seen from (9), the measurement of LDV can increase the observability of attitude, and velocity which indirectly affects the position accuracy. According to (9), the estimated parameters of SINS can be expressed as:

$$\mathbf{X}_{1D-LDV} = [\phi_{mx} \quad \phi_{mz} \quad \delta K]^T \quad (10)$$

where the ϕ_{my} is disregarded, as it is unobservable for SINS/1D-LDV integrated navigation system.

2.3. SINS/GNSS/1D-LDV integrated system

Due to the inherent weakness of GNSS signals and the time-accumulated errors of a stand-alone SINS, the SINS/GNSS integrated navigation system cannot maintain a reliable positioning solution in challenging environments. To improve the reliability and accuracy of the system, 1D-LDV is introduced in addition to SINS/GNSS integration to form a SINS/GNSS/1D-LDV integrated navigation system. Since 1D-LDV can provide accurate velocity information, it can prevent the divergence of the SINS/GNSS integrated navigation error when GNSS fails.

The state equation and state vector of the integrated navigation system can be expressed as:

$$\dot{\mathbf{X}} = \mathbf{F}\mathbf{X} + \mathbf{G}\mathbf{w} \quad (11)$$

$$\mathbf{X} = [\mathbf{X}_{SINS} \quad \mathbf{X}_{1D-LDV}]^T \quad (12)$$

where \mathbf{X} is the state vector, \mathbf{F} is the 18×18 system state transition matrix, \mathbf{G} is the noise transfer matrix, and \mathbf{w} is the system noise vector.

The measurement equation of the integrated navigation system can be expressed as:

$$\mathbf{Z} = \mathbf{H}\mathbf{X} + \mathbf{v} \quad (13)$$

where \mathbf{H} is the measurement transition matrix, \mathbf{v} is the measurement noise (zero-mean Gaussian white noise), and \mathbf{Z} is the measurement value. The measurement value comprises the velocity and position errors of SINS and the velocity error of 1D-LDV, which can be expressed as:

$$\mathbf{Z} = \begin{bmatrix} \mathbf{v}_{SINS}^n - \mathbf{v}_{GNSS} \\ \mathbf{p}_{SINS} - \mathbf{p}_{GNSS} \\ \mathbf{v}_{LDV}^n - \mathbf{v}_{SINS} \end{bmatrix} \quad (14)$$

where \mathbf{v}_{GNSS} and \mathbf{p}_{GNSS} are the velocity and position outputs of the GNSS.

The measurement transition matrix is given as:

$$H = \begin{bmatrix} \mathbf{0}_{3 \times 3} & \mathbf{I}_3 & \mathbf{0}_{3 \times 3} & \mathbf{0}_{3 \times 6} & \mathbf{0}_{3 \times 2} & \mathbf{0}_{3 \times 1} \\ \mathbf{0}_{3 \times 3} & \mathbf{0}_{3 \times 3} & \mathbf{I}_3 & \mathbf{0}_{3 \times 6} & \mathbf{0}_{3 \times 2} & \mathbf{0}_{3 \times 1} \\ \mathbf{v}^n \times & -\mathbf{I}_3 & \mathbf{0}_{3 \times 3} & \mathbf{0}_{3 \times 6} & \mathbf{C}_b^n \mathbf{C}_v & \mathbf{v}^n \end{bmatrix} \quad (15)$$

where

$$\mathbf{C}_v = \begin{bmatrix} 0 & \mathbf{v}_{(y)}^b \\ \mathbf{v}_{(z)}^b & -\mathbf{v}_{(x)}^b \\ -\mathbf{v}_{(y)}^b & 0 \end{bmatrix}. \quad (16)$$

3. The proposed SINS/GNSS/2D-LDV integrated navigation method

According to (1) and [1], the attitude, velocity, and position information of the navigation system are related to the height information of the system. Therefore, the divergence of the height channel of the navigation system will inevitably affect the positioning accuracy of the vehicle. Hence, it is crucial to ensure the accuracy of the height information when the GNSS signal fails. In addition, position information is a 3D information, and its measurement accuracy naturally needs to include height accuracy. Although in most occasions, researchers are more concerned about the horizontal positioning accuracy of the navigation system, but for UGVs in cities with large altitude differences, such as Chongqing, China, there is an urgent need for high-accuracy height information. Moreover, accurate height information is also a must for UGVs used for surveying and mapping.

The SINS/GNSS/1D-LDV integrated navigation model is analogous to the SINS/GNSS/OD integrated navigation model, which is a widely used integrated navigation model today. Although the 1D-LDV has many advantages over the OD, it has a limitation as a 1D velocity sensor: it does not provide effective long-term altitude error suppression in integrated navigation systems when GNSS is unavailable for long periods of time. In this section, an SINS/GNSS/2D-LDV integrated navigation method is proposed to further improve the reliability of the UGV.

3.1. SINS/2D-LDV tightly coupled model

Theoretically, LDV requires only two intersecting measurement beams to obtain 2D velocity information. The literature [32] describes a vehicle-based 2D-LDV that consists of two 1D LDVs with a reference optical structure. However, this structure is bulky and expensive, limiting its further application in the field of integrated navigation. Literature [33] designed a pitch-independent LDV based on a dual measurement beam to eliminate the influence of vehicle pitch on vehicle-based LDV. This optical structure is modified from a 1D LDV with a reference optical structure, adding only a beam splitter and a full mirror to the optics. Therefore, it is very compact. In recent years, pitch-independent LDVs have been used in the field of land integrated navigation to provide high-precision pitch-independent 1D velocities for SINS. In

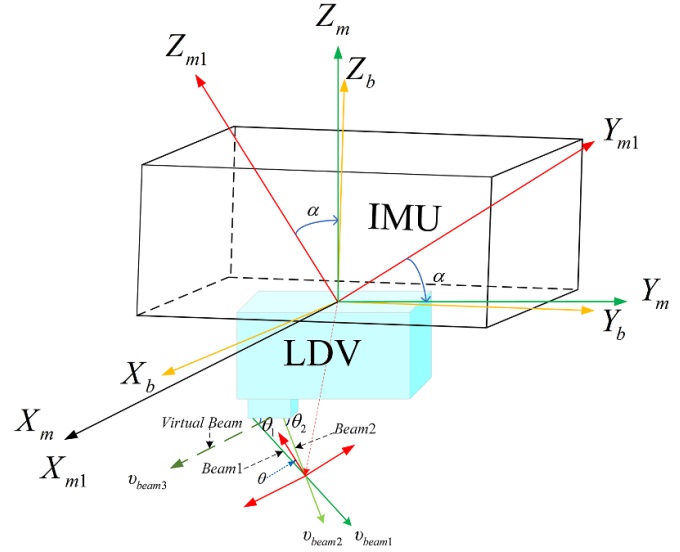


Figure 2. Installation relationship of the 2D-LDV and IMU in the tightly coupled model.

this section, the pitch-independent LDV is used as a 2D-LDV and a tightly coupled model of the SINS/2D-LDV is presented.

Figure 2 illustrates the specific installation relationship between the IMU and the LDV, especially the relationship between the coordinate systems of IMU and LDV. $X_b, Y_b,$ and Z_b are the three axes of the IMU frame (b frame). X_{m1}, Y_{m1} and Z_{m1} are three orthogonal axes that define the initial frame of the LDV ($m1$ frame). The $m1$ frame is established by the following procedure: the Z_{m1} axis coincides with the angle bisector of the two incident beams and points upward; the Y_{m1} axis lies in the plane of the two incident beams and is orthogonal to the Z_{m1} axis, pointing forward; and the X_{m1} axis is determined by the right-hand rule. $X_m, Y_m,$ and Z_m are the three axes of the LDV frame (m frame). $Beam1$ and $Beam2$ are the two measurement beams of the LDV, and v_{beam1} and v_{beam2} are the corresponding sub-velocities along the beam direction measured by each beam. θ_1 and θ_2 are the designed inclination angles of $Beam1$ and $Beam2$, respectively, and $\theta_1, \theta_2 \in [0^\circ \ 180^\circ]$. θ is the included angle between the angle bisector of the two incident beams and two incident beams.

Since the 2D-LDV can measure velocity information in two dimensions, the velocity of the 2D-LDV in the $m1$ frame can be expressed as

$$\mathbf{v}_{LDV}^{m1} = [0 \quad v'_{LDV-y} \quad v'_{LDV-z}]^T \quad (17)$$

where v'_{LDV-y} and v'_{LDV-z} are the forward and vertical velocities of the 2D-LDV in the $m1$ frame, respectively.

According to the definition of the $m1$ frame, the relationship between the velocity in the $m1$ frame and the velocities measured by the two outgoing beams of the 2D-LDV is as follows

$$v'_{LDV-y} \sin \theta - v'_{LDV-z} \cos \theta = v_{beam1} \quad (18)$$

$$-v'_{LDV-y} \sin \theta - v'_{LDV-z} \cos \theta = v_{beam2}. \quad (19)$$

In the SINS/2D-LDV tightly coupled method, the sub-velocities measured by each of the two 2D-LDV beams are used directly, instead of the 2D velocities derived from them. Since both 1D-LDV and 2D-LDV require the use of non-holonomic constraints for three-dimensional velocity measurements, a virtual beam along the X_m axis with a zero-output value is introduced as a lateral constraint in the SINS/2D-LDV tightly coupled method. v_{beam3} is the velocity along the direction of the virtual beam, and $v_{beam3} = 0$. The beam frame is defined by *Beam1*, *Beam2* and virtual beam. Using equations (18) and (19), together with the constructed virtual beam and velocity, the transformation relationship between the velocity in the beam frame and the 2D velocity of 2D-LDV in the m frame is as follows:

$$\begin{bmatrix} v_{beam1} \\ v_{beam2} \\ v_{beam3} \end{bmatrix} = \mathbf{v}_{LDV}^{beam} = \mathbf{C}_{m1}^{beam} \mathbf{v}_{LDV}^{m1} \quad (20)$$

where

$$\begin{aligned} \mathbf{C}_{m1}^{beam} &= \begin{bmatrix} 0 & \sin \theta & -\cos \theta \\ 0 & -\sin \theta & -\cos \theta \\ 1 & 0 & 0 \end{bmatrix} + \begin{bmatrix} 0 & \cos \theta & \sin \theta \\ 0 & -\cos \theta & \sin \theta \\ 0 & 0 & 0 \end{bmatrix} \Delta \theta \\ &= \mathbf{C}_B + \mathbf{C}_{dB} \Delta \theta \end{aligned} \quad (21)$$

where $\Delta \theta$ is the deviation between the design value of θ and the real value of θ .

When the two measurement beams of the 2D-LDV are asymmetrical about the Z_m axis in the outgoing direction, the $m1$ frame has a rotational relationship with the m frame, with the X_m axis as the axis of rotation. Therefore, the velocity vector of the 2D-LDV in the m frame can be written as

$$\mathbf{v}_{LDV}^m = \mathbf{C}_{\alpha x} \mathbf{v}_{LDV}^{m1} = \begin{bmatrix} 0 \\ v'_{LDV-y} \cos \alpha - v'_{LDV-z} \sin \alpha \\ v'_{LDV-y} \sin \alpha + v'_{LDV-z} \cos \alpha \end{bmatrix} \quad (22)$$

where $\mathbf{C}_{\alpha x}$ is the elementary rotation matrix along the X_m axis, and $\mathbf{C}_{\alpha x}$ can be expressed as

$$\mathbf{C}_{\alpha x} = \begin{bmatrix} 1 & 0 & 0 \\ 0 & \cos \alpha & -\sin \alpha \\ 0 & \sin \alpha & \cos \alpha \end{bmatrix} \quad (23)$$

where α is the rotation angle from the $m1$ frame to the m frame, and $\alpha = \frac{\pi - (\theta_1 + \theta_2)}{2}$.

According to (20) and (22), the relationship between the beam frame and the m frame can be obtained. Therefore, based on the above discussion, the projection of the velocity of the SINS in the beam frame is:

$$\mathbf{v}_{SINS}^{beam} = \mathbf{C}_{m1}^{beam} \mathbf{C}_{\alpha x}^T \mathbf{C}_b^m (\mathbf{I}_3 + \phi_m \times) \mathbf{C}_n^b (\mathbf{I}_3 + \varphi \times) \mathbf{v}_{SINS}^n \quad (24)$$

Due to the excellent performance of the LDV, the deviation of v_{beam1} and v_{beam2} from the true velocities is not considered in this paper.

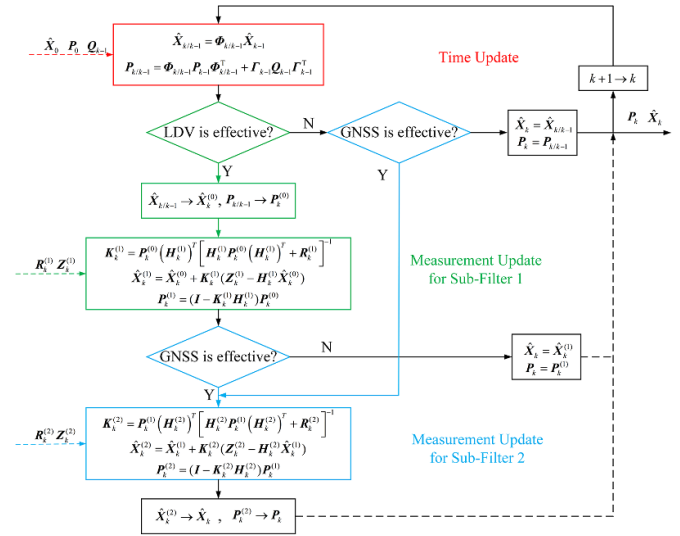


Figure 3. Kalman filter scheme for SINS/GNSS/2D-LDV integration.

For the SINS/2D-LDV integrated navigation model, the velocity observation can be written as

$$\begin{aligned} \mathbf{v}_{LDV}^{beam} - \mathbf{v}_{SINS}^{beam} &= \mathbf{v}_{LDV}^{beam} - \mathbf{C}_{m1}^{beam} \mathbf{C}_{\alpha x}^T \mathbf{C}_b^m (\mathbf{I}_3 + \phi_m \times) \\ &\quad \times \mathbf{C}_n^b (\mathbf{I}_3 + \varphi \times) \mathbf{v}_{SINS}^n \\ &\approx \mathbf{C}_B \mathbf{C}_{\alpha x}^T \mathbf{C}_b^m \mathbf{C}_n^b (\mathbf{v}^n \times) \varphi + \mathbf{C}_B \mathbf{C}_{\alpha x}^T \mathbf{C}_b^m (\mathbf{v}^b \times) \phi_m \\ &\quad - \mathbf{C}_{dB} \mathbf{C}_{\alpha x}^T \mathbf{C}_b^m \mathbf{C}_n^b \mathbf{v}^n \Delta \theta - \mathbf{C}_B \mathbf{C}_{\alpha x}^T \mathbf{C}_b^m \mathbf{C}_n^b \delta \mathbf{v}_{SINS}^n \end{aligned} \quad (25)$$

According to (25), the $\Delta \theta$ and ϕ_m are set as the parameter to be estimated for the 2D-LDV:

$$\mathbf{X}_{2D-LDV} = [\phi_{mx} \quad \phi_{my} \quad \phi_{mz} \quad \Delta \theta]^T \quad (26)$$

3.2. SINS/GNSS/2D-LDV integrated scheme

For the SINS/GNSS/LDV integrated navigation system, the data output frequencies of the three sensors are often inconsistent. Taking the sensor used in this paper as an example: the data output frequency of SINS, LDV, and GNSS is 200 HZ, 100 HZ, and 10 HZ, respectively. The output of the three sensors is not synchronized, especially, GNSS has a much lower frequency than SINS and LDV. Therefore, it is difficult to achieve SINS/GNSS/LDV integration with a traditional Kalman filter, and most of the LDV data will not be used. This will affect the accuracy of the SINS/GNSS/LDV integrated navigation system, especially when SINS uses a low-cost IMU. To solve this problem, we construct an asynchronous Kalman filter with two sub-filters based on the idea of sequential Kalman filtering. Figure 3 illustrates the filter flowchart of the SINS/GNSS/LDV integrated navigation system.

As shown in figure 3, the asynchronous Kalman filter based on SINS/GNSS/LDV integration consists of four steps. First, when both LDV and GNSS data are unavailable, only the time update is performed. Second, when LDV data is available and

GNSS data is unavailable, the time update and the measurement update of sub-filter 1 are performed sequentially. Third, when LDV data is unavailable and GNSS data is available, the time update and the measurement update of sub-filter 2 are performed sequentially. Finally, when both LDV data and GNSS data are available, the time update, the measurement update of sub-filter 1 and the measurement update of sub-filter 2 are performed sequentially. This asynchronous Kalman filter can integrate sensor information from three different frequencies of SINS, GNSS and LDV effectively.

According to (2) and (26), the system state vector of the proposed SINS/GNSS/2D-LDV integrated navigation method is

$$\mathbf{X} = [\mathbf{X}_{\text{SINS}} \quad \mathbf{X}_{\text{2D-LDV}}]^T. \quad (27)$$

Given the excellent performance of the internal lasers of 2D-LDV and the fixed installation relationship between the 2D-LDV and the SINS, the error of included angle of beam of 2D-LDV and the error of the misalignment angles between the m frame and the b frame are modeled as random constants in the current SINS/GNSS/2D-LDV integrated navigation system. Therefore, the following error equations are obtained:

$$\dot{\mathbf{X}}_{\text{2D-LDV}} = \begin{bmatrix} \dot{\phi}_{mx} \\ \dot{\phi}_{my} \\ \dot{\phi}_{mz} \\ \Delta\theta \end{bmatrix} = \begin{bmatrix} 0 \\ 0 \\ 0 \\ 0 \end{bmatrix}. \quad (28)$$

According to (1) and (28), the state equation of the proposed SINS/GNSS/2D-LDV integrated navigation method is established as follows:

$$\dot{\mathbf{X}} = \begin{bmatrix} \mathbf{F}_{\text{SINS}} & \mathbf{0}_{15 \times 4} \\ \mathbf{0}_{4 \times 15} & \mathbf{0}_{4 \times 4} \end{bmatrix} \mathbf{X} + \begin{bmatrix} -\mathbf{C}_b^m & \mathbf{0}_{3 \times 3} \\ \mathbf{0}_{3 \times 3} & \mathbf{C}_b^m \\ \mathbf{0}_{13 \times 3} & \mathbf{0}_{13 \times 3} \end{bmatrix} \begin{bmatrix} \varepsilon_{wx} \\ \varepsilon_{wy} \\ \varepsilon_{wz} \\ \nabla_{wx} \\ \nabla_{wy} \\ \nabla_{wz} \end{bmatrix} \quad (29)$$

where ε_{wi} and $\nabla_{wi}(i = x, y, z)$ denote the noise of the gyro and accelerometer, respectively. \mathbf{F}_{SINS} is the 15×15 state transition matrix based on (1).

The measurement equation of the proposed SINS/GNSS/2D-LDV integrated navigation method is established as follows:

$$\begin{cases} \mathbf{Z}_1 = \mathbf{H}_1 \mathbf{X} + \mathbf{v}_1 \\ \mathbf{Z}_2 = \mathbf{H}_2 \mathbf{X} + \mathbf{v}_2 \end{cases} \quad (30)$$

where \mathbf{H}_1 and \mathbf{H}_2 are the measurement transition matrices of sub-filter 1 and sub-filter 2, respectively. \mathbf{v}_1 and \mathbf{v}_2 represent the measurement noise (zero-mean Gaussian white noise) for sub-filter 1 and sub-filter 2, respectively. \mathbf{Z}_1 and \mathbf{Z}_2 denote the measurement values for sub-filter 1 and sub-filter 2, respectively.

3.3. Measurement update for sub-filter 1

In this section, the measurement update process for sub-filter 1 using velocity observation is given. Based on (25), the measurement value and measurement transition matrix of sub-filter 1 is

$$\mathbf{Z}_1 = \mathbf{v}_{\text{LDV}}^{\text{beam}} - \mathbf{v}_{\text{SINS}}^{\text{beam}} \quad (31)$$

$$\mathbf{H}_1 = \begin{bmatrix} \mathbf{C}_B \mathbf{C}_{\alpha x}^T \mathbf{C}_b^m \mathbf{C}_n^b (\mathbf{v}^n \times) & -\mathbf{C}_B \mathbf{C}_{\alpha x}^T \mathbf{C}_b^m \mathbf{C}_n^b & \mathbf{0}_{3 \times 9} \\ \mathbf{C}_B \mathbf{C}_{\alpha x}^T \mathbf{C}_b^m (\mathbf{v}^b \times) & -\mathbf{C}_{dB} \mathbf{C}_{\alpha x}^T \mathbf{C}_b^m \mathbf{C}_n^b \mathbf{v}^n & \end{bmatrix}. \quad (32)$$

The Kalman filter is optimal only when the LDV measurement noise follows a zero-mean Gaussian distribution. However, if the measurement value of LDV contains outliers, the optimal assumptions of the Kalman filter are violated. This can affect the normal working state of the filter. To reduce the impact of outliers from the LDV on the Kalman filter, the Mahalanobis distance of the innovation vector is introduced to detect the outliers of LDV and isolate the outliers when they occur. The Mahalanobis distance denotes the distance between two vectors and can be expressed as

$$M(\mathbf{a}, \mathbf{b}) = \sqrt{(\mathbf{a} - \mathbf{b})^T \Sigma^{-1} (\mathbf{a} - \mathbf{b})} \quad (33)$$

where Σ is the covariance matrix.

If the innovation vector has a Gaussian distribution, its Mahalanobis distance should follow a chi-square distribution with the same degrees of freedom as the dimension of the innovation vector

$$f_{1,k} = \mathbf{e}_{1,k}^T [\mathbf{H}_{1,k} \mathbf{P}_{k|k-1} \mathbf{H}_{1,k}^T + \mathbf{R}_{1,k}]^{-1} \mathbf{e}_{1,k} \sim \chi^2(n) \quad (34)$$

where the subscript k is the time index, $\mathbf{P}_{k|k-1}$ denotes the one-step prediction covariance matrix at time k , $\mathbf{H}_{1,k}$ is the measurement transition matrix of sub-filter 1 at time k , $\mathbf{R}_{1,k}$ is the measurement noise covariance matrix of sub-filter 1 at time k , and $\mathbf{e}_{1,k}$ is the innovation vector of sub-filter 1 at time k , defined as

$$\mathbf{e}_{1,k} = \mathbf{Z}_{1,k} - \mathbf{H}_{1,k} \mathbf{X}_{k|k-1} \quad (35)$$

where $\mathbf{Z}_{1,k}$ is the measurement value of sub-filter 1 at time k , and $\mathbf{X}_{k|k-1}$ is the one-step prediction state vector at time k .

Based on (35), the judgment criterion is defined as:

$$\begin{cases} f_{1,k} \leq T_D & \text{Normal} \\ f_{1,k} > T_D & \text{Abnormal} \end{cases} \quad (36)$$

where T_D is the predefined threshold and can be determined by the degrees of freedom and the desired significance level of the chi-square distribution.

3.4. Measurement update for sub-filter 2

In this section, the measurement update process for sub-filter 2 using both velocity and position observations is given. The measurement value \mathbf{Z}_2 is given as follows:

$$\mathbf{Z}_2 = \begin{bmatrix} \mathbf{v}_{\text{SINS}}^n - \mathbf{v}_{\text{GNSS}} \\ \mathbf{p}_{\text{SINS}} - \mathbf{p}_{\text{GNSS}} \\ \mathbf{v}_{\text{LDV}}^{\text{beam}} - \mathbf{v}_{\text{GNSS}}^{\text{beam}} \end{bmatrix} \quad (37)$$

where $\mathbf{v}_{\text{LDV}}^{\text{beam}} - \mathbf{v}_{\text{GNSS}}^{\text{beam}}$ is used to calibrate the error term in $\mathbf{X}_{2\text{D-LDV}}$ and can be written as:

$$\begin{aligned} \mathbf{v}_{\text{LDV}}^{\text{beam}} - \mathbf{v}_{\text{GNSS}}^{\text{beam}} &= \mathbf{v}_{\text{LDV}}^{\text{beam}} - \mathbf{C}_{m1}^{\text{beam}} \mathbf{C}_{\alpha x}^{\text{T}} \mathbf{C}_b^m (\mathbf{I}_3 + \phi_m \times) \\ &\quad \times \mathbf{C}_n^b (\mathbf{I}_3 + \varphi \times) \mathbf{v}_{\text{GNSS}} \\ &\approx \mathbf{C}_B \mathbf{C}_{\alpha x}^{\text{T}} \mathbf{C}_b^m \mathbf{C}_n^b (\mathbf{v}_{\text{GNSS}} \times) \varphi \\ &\quad + \mathbf{C}_B \mathbf{C}_{\alpha x}^{\text{T}} \mathbf{C}_b^m (\mathbf{v}_{\text{GNSS}}^b \times) \phi_m \\ &\quad - \mathbf{C}_{dB} \mathbf{C}_{\alpha x}^{\text{T}} \mathbf{C}_b^m \mathbf{C}_n^b \mathbf{v}_{\text{GNSS}} \Delta \theta \end{aligned} \quad (38)$$

where $\mathbf{v}_{\text{GNSS}}^b$ is the projection of the GNSS output velocity in the b frame.

The measurement transition matrix of sub-filter 2 is given as

$$\mathbf{H}_2 = \begin{bmatrix} \mathbf{0}_{6 \times 3} & \mathbf{C}_B \mathbf{C}_{\alpha x}^{\text{T}} \mathbf{C}_b^m \mathbf{C}_n^b (\mathbf{v}_{\text{GNSS}} \times) \\ \mathbf{I}_6 & \mathbf{0}_{3 \times 6} \\ \mathbf{0}_{6 \times 6} & \mathbf{0}_{3 \times 6} \\ \mathbf{0}_{6 \times 3} & \mathbf{C}_B \mathbf{C}_{\alpha x}^{\text{T}} \mathbf{C}_b^m (\mathbf{v}_{\text{GNSS}}^b \times) \\ \mathbf{0}_{6 \times 1} & -\mathbf{C}_{dB} \mathbf{C}_{\alpha x}^{\text{T}} \mathbf{C}_b^m \mathbf{C}_n^b \mathbf{v}_{\text{GNSS}} \end{bmatrix}^{\text{T}}. \quad (39)$$

To ensure the validity of GNSS signals, a two-step method is applied in scenarios where GNSS and SINS are loosely coupled, i.e., where the position and velocity information output from GNSS is used directly. First, the GNSS status information, which is output by almost all GNSS receivers, is used as a simple criterion to determine whether the GNSS signal is valid or not. Second, the same method as for sub-filter 1 is used to further identify the GNSS outliers. If the GNSS measurement value is considered an outlier, sub-filter 2 is not run.

4. Vehicle-mounted field test

To evaluate the practical value and effectiveness of the proposed SINS/GNSS/2D-LDV integration method, two groups of long-distance, high-mobility land vehicle tests are carried out, including different driving environments such as open-sky, urban canyons, tunnels, viaducts and boulevards. As shown in figure 4, the test equipment in this paper includes: a self-developed high-precision IMU, a medium-precision IMU, a self-made pitch-independent LDV, and a dual-antenna GNSS receiver. The high-precision IMU (100 Hz) consists of three high-precision ring laser gyros with a bias instability of $0.005^\circ \text{ h}^{-1}$ and a random walk of $0.0008^\circ \sqrt{\text{h}^{-1}}$, and three high-precision quartz accelerometers with a bias instability of $20 \mu\text{g}$ and a random walk of $10 \mu\text{g} \sqrt{\text{h}^{-1}}$. The medium-precision IMU (200 Hz) consists of three ring laser gyros with

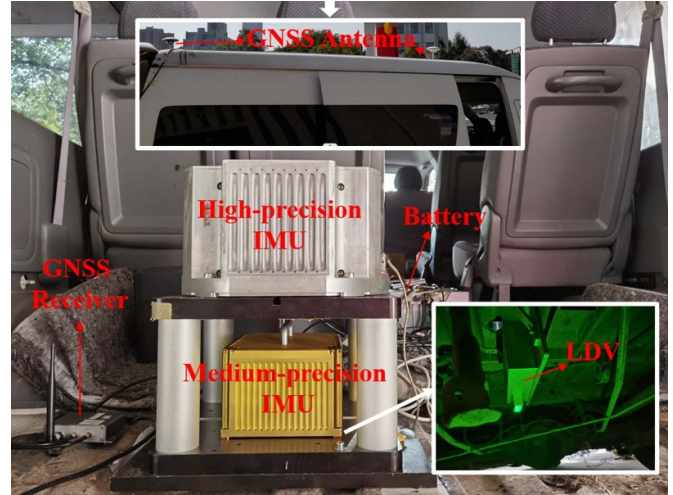


Figure 4. Installation diagram of the experimental system.

a bias instability of $0.03^\circ \text{ h}^{-1}$ and three quartz accelerometers with a bias instability of $50 \mu\text{g}$. The LDV (100 Hz) has a velocity measurement error of $0.1\% (1\sigma)$. The GNSS (10 Hz) has a horizontal positioning accuracy and an altitude accuracy of 0.1 m.

Two groups of field tests were conducted in Hunan Province, China. At the start point, the vehicle remained stationary for about 13 min before moving. During this time, static attitude alignment was performed to obtain an accurate initial attitude. The high-precision IMU was used for reference and the medium-precision IMU was used for system testing. The reference position of the vehicle is provided by the high-precision SINS/GNSS integrated navigation system, which integrates a high-precision IMU and a differential GNSS, and uses the Rauch-Tung-Striebel smoothing algorithm to process the data.

The movement trajectory and the LDV output of the first vehicle test are shown in figure 5, and the test lasted approximately 2.08 h with a total distance of 151.9 km. Figure 6 shows the number of satellites and the GNSS working status during the first vehicle test. The operating states of the differential GNSS are as follows: State 4 indicates that GNSS outputs a fixed solution with the highest accuracy, generally within 0.1 m; State 5 indicates that GNSS outputs a floating-point solution with higher accuracy, generally within 3 m; State 2 and State 1 indicate that GNSS outputs a differential solution and a single point solution respectively, with lower accuracy, generally greater than 5 m; State 0 indicates that GNSS fails, with no satellite data received. As is shown in figure 5, in the first vehicle test, the vehicle travelled a long distance and maintained a velocity greater than 20 m s^{-1} for most of the time, indicating that this was a long-distance, high-mobility experiment. Figure 6 shows that the GNSS signal experienced frequent failures and interference during this experiment. These challenges were not intentionally selected by the experimenters, but rather occurred naturally and frequently in practice. They represent a common problem that future UGVs will have to deal with.

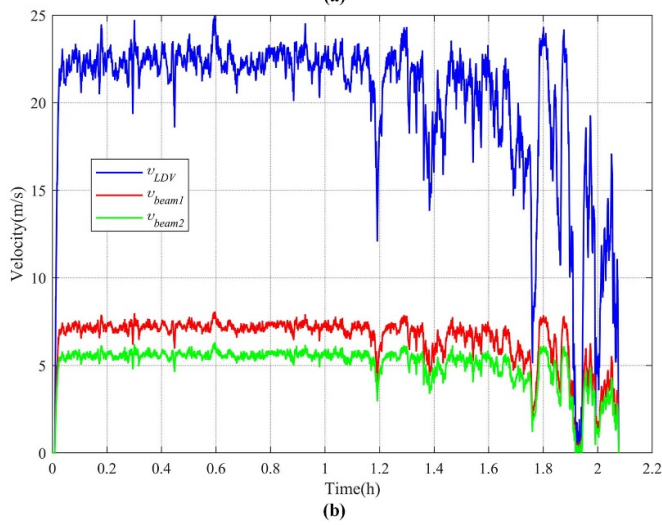
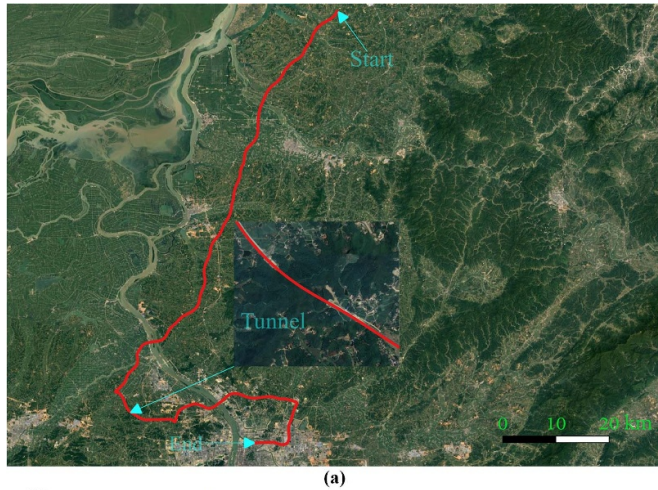


Figure 5. (a) Trajectory of the vehicle in the first field test. (b) Velocity curve of LDV output in the first field test.

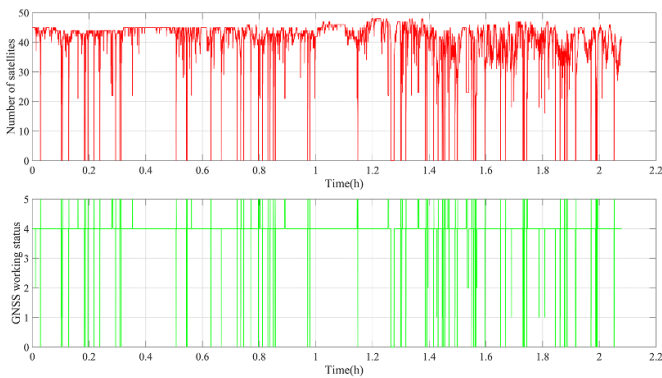


Figure 6. The number of satellites and the GNSS working status during the first vehicle test.

Figure 7 shows the parameter of the 2D-LDV estimated by proposed method in the first vehicle test. As seen from figure 7, both the included angle between the two beams of the 2D-LDV and the pitch and heading misalignment angles between the m frame and the b frame can be estimated and converge rapidly, while the roll misalignment angle between the m frame

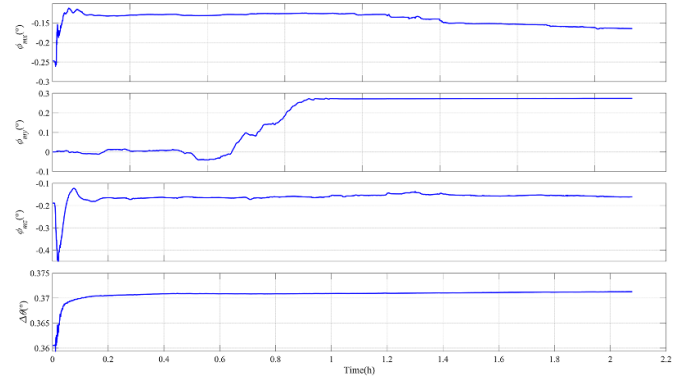


Figure 7. The parameter estimation results for the 2D-LDV in the first vehicle test.

and the b frame converges slowly. This is because the vehicle maneuvers on the y -axis are much larger than those on the x -axis and z -axis during the terrestrial vehicle test. Therefore, for the terrestrial SINS/2D-LDV integrated navigation system, the roll misalignment angle between the m frame and the b frame has weak observability in practical application. Moreover, since the roll misalignment angle between the m frame and the b frame is usually small and causes little velocity error, it can be ignored in practical application.

The SINS/GNSS integrated navigation system relies on GNSS information, which is unavailable in highly shielded environments such as tunnels. In such cases, the system degenerates into a pure inertial system, and the navigation errors accumulate rapidly over time. LDVs can help solve this problem by providing velocity measurements. Figures 8 and 9 show the performance of the SINS/LDV system in a GNSS-denied environment. Here, SINS denotes pure inertial navigation, SINS/1D-LDV uses the method introduced in section 2 of this paper, SINS/2D-LDV (tightly coupled) uses the tightly coupled model proposed in this paper, and SINS/2D-LDV (loosely coupled) uses the method proposed in the [32]. The results in figures 8 and 9 show that the SINS/LDV integrated navigation can effectively suppress the divergence of error of SINS. Moreover, the SINS/2D-LDV integrated navigation has higher positioning accuracy than SINS/1D-LDV integrated navigation under the same conditions, especially in height, which can better help UGV complete its navigation tasks in the absence of satellite information. It is worth mentioning that there is no significant difference in positioning accuracy between the SINS/2D-LDV loosely coupled method and the SINS/2D-LDV tightly coupled method when the LDV output is normal. To test the robustness of the proposed SINS/2D-LDV tightly coupled method, we manipulated the LDV output data of test 1 by human intervention, in which the LDV $beam1$ signal was ‘interrupted’ for 1 and 2 s at 1327s and 5167s, and the LDV $beam2$ signal was ‘interrupted’ for 2 s at 2667s respectively, to simulate the short-term loss of one LDV beam signal during the vehicle’s motion. The positioning results of SINS/2D-LDV loosely coupled method and SINS/2D-LDV tightly coupled method with multiple interruptions of one LDV beam signal are shown in figure 10.

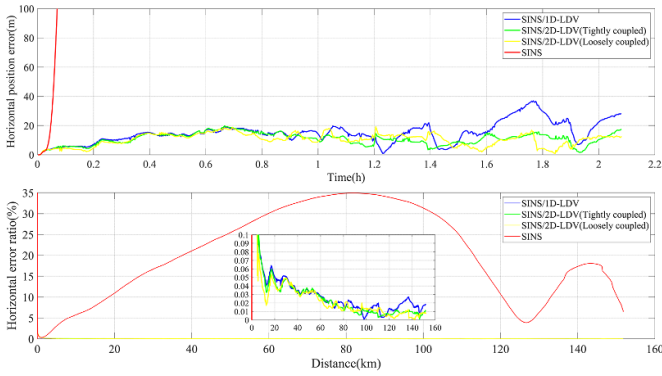


Figure 8. Horizontal position error of SINS/LDV and SINS in the first vehicle test.

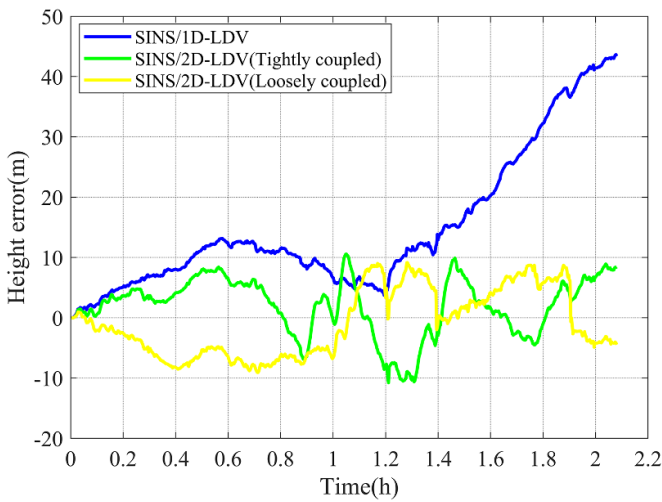


Figure 9. Height error of SINS/LDV in the first vehicle test.

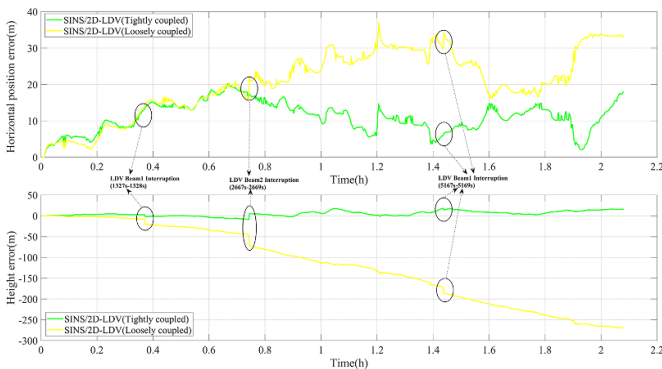


Figure 10. The positioning result of the SINS/2D-LDV loosely coupled method and the SINS/2D-LDV tightly coupled method under multiple interruptions of one LDV beam signal in the first vehicle test.

As shown in figure 10, the traditional SINS/2D-LDV loosely coupled method does not cope well with this situation when the individual LDV beams are lost for a short period of time, and its height error is rapidly diverged, and the horizontal positioning accuracy is also affected to a certain extent, whereas the SINS/2D-LDV tightly coupled method

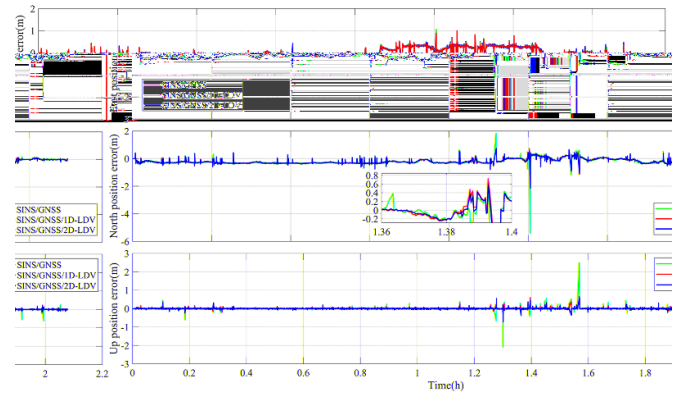


Figure 11. Comparison of North, East and Up positioning errors during the first vehicle test.

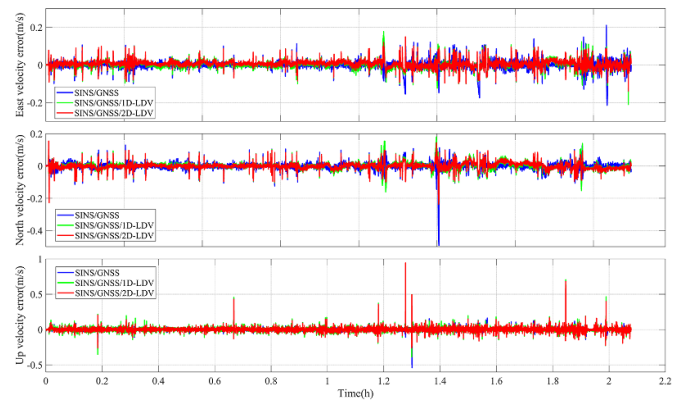


Figure 12. Comparison of North, East and Up velocity errors during the first vehicle test.

proposed in this paper is almost unaffected. The reason for this difference is that the LDV velocity information used in the SINS/2D-LDV loosely coupled method is calculated from the measurement value of the two beams of the LDV, and its accuracy depends on the accuracy of the two beams together, while the SINS/2D-LDV tightly coupled method directly uses the measurement value of the two beams of the LDV, and when a single beam measurement is unavailable, the measurement value of the other beam can still suppress errors in the integrated navigation.

Figures 11–13 show the position error, velocity error, and attitude error of SINS/GNSS, SINS/GNSS/1D-LDV, and SINS/GNSS/2D-LDV in the first vehicle test to evaluate the performance of the proposed SINS/GNSS/2D-LDV method. Table 1 summarizes the root mean square error (RMSE) of the position error, velocity error, and attitude error shown in figures 11–13.

Figures 11–13 and table 1 show that by adding LDV to the SINS/GNSS integrated navigation system, the whole navigation system has stronger environmental adaptability and reliability, and SINS/GNSS/1D-LDV and SINS/GNSS/2D-LDV improve the positioning accuracies of the east, north, and vertical components by (17.52%, 12.48%, 58.59%) and (18.56%, 12.62%, 61.63%), respectively, compared with SINS/GNSS. The SINS/GNSS/LDV integrated navigation system can

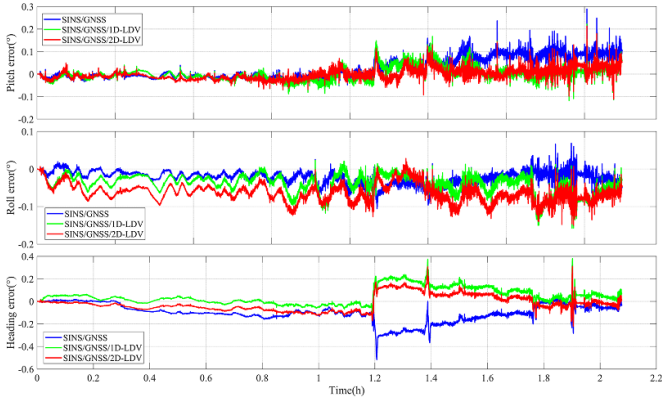


Figure 13. Comparison of attitude errors during the first vehicle test.

Table 1. Statistical result of navigation error in the first test.

RMSE		SINS/GNSS	SINS/GNSS/ 1D-LDV	SINS/GNSS/ 2D-LDV
Position Error (m)	E	0.2403	0.1982	0.1957
	N	0.2885	0.2525	0.2521
	U	0.1053	0.0436	0.0404
Velocity Error (m s ⁻¹)	E	0.0252	0.0229	0.0209
	N	0.0276	0.0246	0.0220
	U	0.0265	0.0257	0.0238
Attitude Error (°)	P	0.0530	0.0302	0.0252
	R	0.0284	0.0459	0.0674
	H	0.1296	0.0843	0.0715

Note: Bold indicates the optimal value.

maintain higher positioning accuracy in the GNSS-denied environment than the commonly used SINS/GNSS integrated navigation system. Furthermore, the SINS/GNSS/LDV integrated navigation system also has lower velocity and attitude errors than the commonly used SINS/GNSS integrated navigation system, especially for heading angle estimation, which is one of the reasons for the improved positioning accuracy. The advantages of the SINS/GNSS/2D-LDV integrated navigation system over the SINS/GNSS/1D-LDV integrated navigation system are mainly in the estimation of height and upward velocity when GNSS fails. Another advantage is the higher robustness of the tightly coupled scheme of 2D-LDV and SINS used in this paper, which effectively suppresses the influence of individual beam measurement errors in both LDV beams on the integrated navigation system.

To further verify the effectiveness and to evaluate the accuracy of the proposed SINS/GNSS/2D-LDV integrated navigation method, the second vehicle test was carried out. The movement trajectory and the LDV output of the second vehicle test are shown in figure 14. The test lasted approximately 1.64 h with a total distance of 121.3 km. The position error, velocity error, and attitude error of SINS/GNSS, SINS/GNSS/1D-LDV, and SINS/GNSS/2D-LDV in the second vehicle test are shown in figures 15–17, and the RMSE of these errors are summarized in table 2.

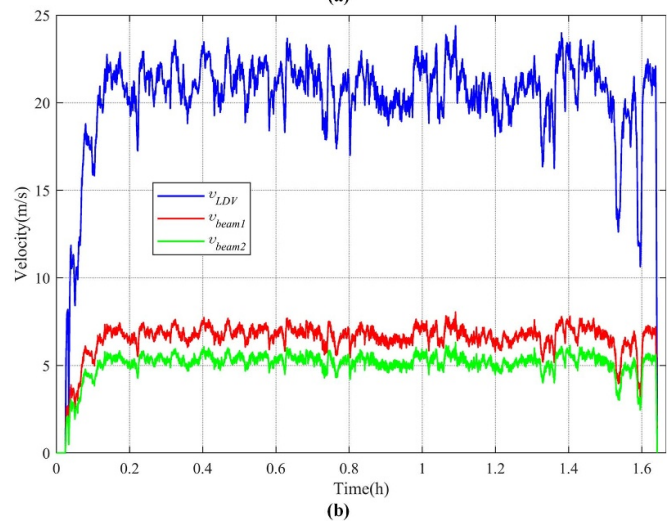
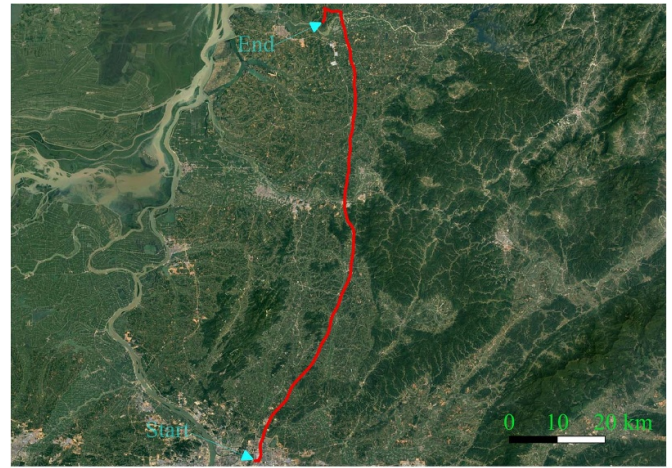


Figure 14. (a) Trajectory of the vehicle in the second field test. (b) Velocity curve of LDV output in the second field test.

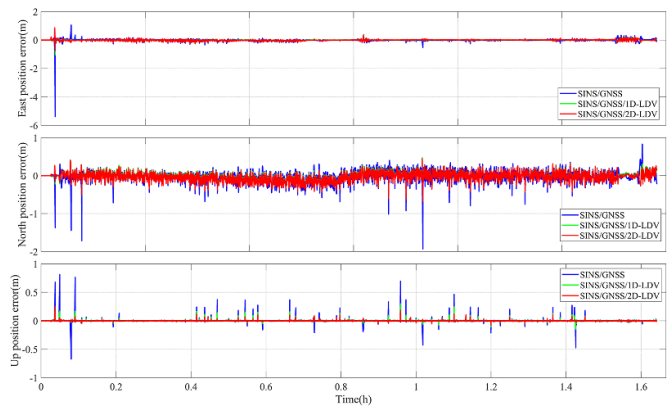


Figure 15. Comparison of North, East and Up positioning errors during the second vehicle test.

Figures 15–17 and table 2 show that the three methods have similar performance in the second experiment as in the first experiment. This further demonstrates the superiority of the SINS/GNSS/2D-LDV integrated navigation.

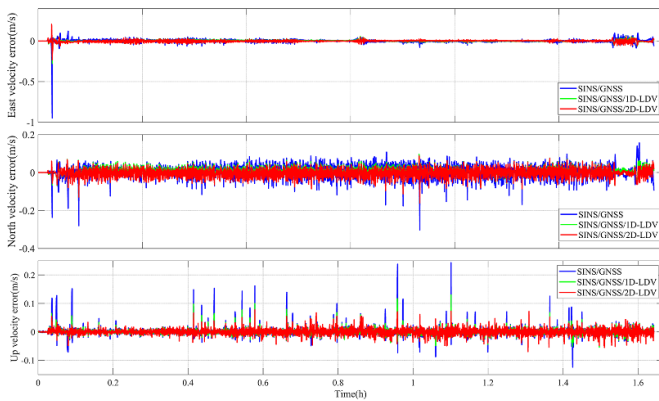


Figure 16. Comparison of North, East and Up velocity errors during the second vehicle test.

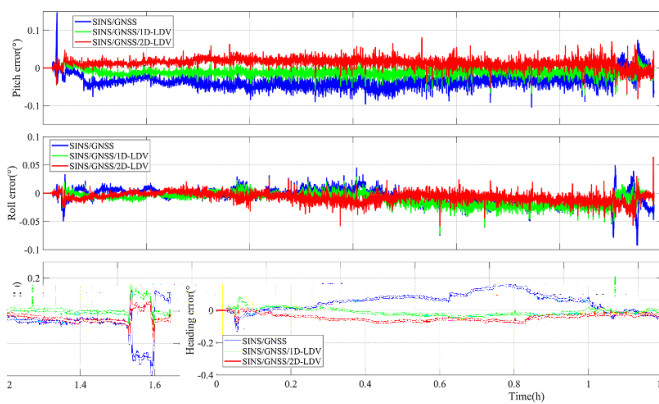


Figure 17. Comparison of attitude errors during the second vehicle test.

Table 2. Statistical result of navigation error in the second test.

RMSE		SINS/GNSS	SINS/GNSS/ 1D-LDV	SINS/GNSS/ 2D-LDV
Position Error (m)	E	0.1158	0.0496	0.0492
	N	0.1449	0.1144	0.1084
	U	0.0436	0.0158	0.0107
Velocity Error (m s ⁻¹)	E	0.0244	0.0124	0.0116
	N	0.0317	0.0219	0.0212
	U	0.0164	0.0106	0.0097
Attitude Error (°)	P	0.0390	0.0148	0.0179
	R	0.0152	0.0144	0.0109
	H	0.0905	0.0293	0.0396

Note: Bold indicates the optimal value.

Compared with the traditional SINS/GNSS integrated navigation method, SINS/GNSS/1D-LDV and SINS/GNSS/2D-LDV achieve improvements of (57.17%, 21.00%, 63.76%) and (57.51%, 25.18%, 75.46%) in the positioning accuracy of the east, north, and vertical components, respectively. The experimental results of the two groups of tests show that adding LDV to the SINS/GNSS integrated navigation system can greatly improve the navigation performance of the system, especially in the height positioning accuracy, which is

improved by more than 50% in both groups of tests. Moreover, adding 2D-LDV to SINS/GNSS can achieve higher navigation performance than adding 1D-LDV, particularly in the height channel. Therefore, the proposed SINS/GNSS/2D-LDV integrated navigation scheme is more suitable for UGVs than SINS/GNSS and SINS/GNSS/1D-LDV (SINS/GNSS/OD).

5. Conclusion

This paper proposes a SINS/GNSS/2D-LDV integrated navigation scheme to meet the need for reliable, continuous and high-precision navigation in UGVs. The effectiveness of the proposed scheme is verified through two groups of long-distance, high-mobility vehicle experiments conducted in multiple challenging environments. The results show that the proposed SINS/GNSS/2D-LDV integrated navigation scheme is reliable and can maintain high horizontal and vertical positioning accuracy even when GNSS is not working properly. Therefore, the proposed scheme can provide reliable navigation information for UGVs in most scenarios, and can provide a technical reference for future large-scale applications of UGVs. Considering that the IMU used in this paper is a medium-precision IMU, we will further verify the effectiveness of this scheme on a low-cost MEMS IMU in the future.

Data availability statement

The data cannot be made publicly available upon publication due to legal restrictions preventing unrestricted public distribution. The data that support the findings of this study are available upon reasonable request from the authors.

Acknowledgments

This research is supported by the Natural Science Foundation of Hunan Province, China (Grant No. 2021JJ30782), and the Major Basic Autonomous Research Project of the College of Advanced Interdisciplinary Studies, National University of Defense Technology (Grant No. ZDJC19-12).

ORCID iDs

Zhiyi Xiang  <https://orcid.org/0000-0003-1766-2409>
 Jian Zhou  <https://orcid.org/0000-0001-6443-2644>

References

- [1] Titterton D H, Weston J L and Weston J L Electrical Engineers I 1997 *Strapdown Inertial Navigation Technology* (Peter Peregrinus Limited)
- [2] Wang D, Wang B, Huang H, Yao Y and Xu X 2023 Robust filter method for SINS/DVL/USBL tight integrated navigation system *IEEE Sens. J.* **23** 10912–23
- [3] Qian L, Qin F, Li A, Li K and Zhu J 2023 An INS/DVL integrated navigation filtering method against complex underwater environment *Ocean Eng.* **278** 114398
- [4] Groves P D 2008 *Principles of GNSS, Inertial, and Multisensor Integrated Navigation Systems* (Artech House)

- [5] Du S, Huang Y, Lin B, Qian J and Zhang Y 2022 A lie group manifold-based nonlinear estimation algorithm and its application to low-accuracy SINS/GNSS integrated navigation *IEEE Trans. Instrum. Meas.* **71** 1–27
- [6] Xu T, Xu X, Xu D, Zou Z and Zhao H 2022 A new robust filtering method of GNSS/MINS integrated system for land vehicle navigation *IEEE Trans. Veh. Technol.* **71** 11443–53
- [7] Zhao C, Yang Z, Cheng X, Hu J and Hou X 2022 SINS/GNSS integrated navigation system based on maximum versoria filter *Chin. J. Aeronaut.* **35** 168–78
- [8] Sun Y, Li Z, Yang Z, Shao K and Chen W 2022 Motion model-assisted GNSS/MEMS-IMU integrated navigation system for land vehicle *GPS Solut.* **26** 131
- [9] Lyu X, Hu B, Wang Z, Gao D, Li K and Chang L 2022 A SINS/GNSS/VDM integrated navigation fault-tolerant mechanism based on adaptive information sharing factor *IEEE Trans. Instrum. Meas.* **71** 1–13
- [10] Sun R, Zhang Z, Cheng Q and Ochieng W Y 2022 Pseudorange error prediction for adaptive tightly coupled GNSS/IMU navigation in urban areas *GPS Solut.* **26** 28
- [11] Zuo Z, Yang B, Li Z and Zhang T 2022 A GNSS/IMU/vision ultra-tightly integrated navigation system for low altitude aircraft *IEEE Sens. J.* **22** 11857–64
- [12] Li X, Qin Z, Shen Z, Li X, Zhou Y and Song B 2022 A high-precision vehicle navigation system based on tightly coupled PPP-RTK/INS/ odometer integration *IEEE Trans. Intell. Transp. Syst.* **24** 1–12
- [13] Mu M and Zhao L 2023 Improved decentralized GNSS/SINS/odometer fusion system for land vehicle navigation applications *Meas. Sci. Technol.* **34** 035117
- [14] Du X, Wang M, Wu W, Zhou P and Cui J 2023 State transformation extended Kalman filter-based tightly coupled strapdown inertial navigation system/global navigation satellite system/laser Doppler velocimeter integration for seamless navigation of unmanned ground vehicle in urban areas *Int. J. Adv. Robot. Syst.* **20** 172988062311584
- [15] Wu Y, Niu X and Kuang J 2021 A comparison of three measurement models for the wheel-mounted MEMS IMU-based dead reckoning system *IEEE Trans. Veh. Technol.* **70** 11193–203
- [16] Ouyang W, Wu Y and Chen H 2021 INS/odometer land navigation by accurate measurement modeling and multiple-model adaptive estimation *IEEE Trans. Aerosp. Electron. Syst.* **57** 245–62
- [17] Dong J, Ren X, Han S and Luo S 2022 UAV vision aided INS/odometer integration for land vehicle autonomous navigation *IEEE Trans. Veh. Technol.* **71** 4825–40
- [18] Yan M, Wang Z and Zhang J 2022 Online calibration of installation errors of SINS/OD integrated navigation system based on improved NHC *IEEE Sens. J.* **22** 12602–12
- [19] Hu H, Li K, Liang W, Li Q and Xie Z 2023 Kilometer sign positioning-aided INS/odometer integration for land vehicle autonomous navigation *IEEE Sens. J.* **23** 4143–58
- [20] Wang L, Niu X, Zhang T, Tang H and Chen Q 2022 Accuracy and robustness of ODO/NHC measurement models for wheeled robot positioning *Measurement* **201** 111720
- [21] Wen Z, Yang G, Cai Q and Chen T 2023 A novel bluetooth-odometer-aided smartphone-based vehicular navigation in satellite-denied environments *IEEE Trans. Ind. Electron.* **70** 3136–46
- [22] Zhou J, Nie X and Lin J 2014 A novel laser Doppler velocimeter and its integrated navigation system with strapdown inertial navigation *Opt. Laser Technol.* **64** 319–23
- [23] Gao C, Wang Q, Wei G and Long X 2017 A highly accurate calibration method for terrestrial laser doppler velocimeter *IEEE Trans. Instrum. Meas.* **66** 1994–2003
- [24] Fu Q, Liu Y, Liu Z, Li S and Guan B 2018 High-accuracy SINS/LDV integration for long-distance land navigation *IEEE/ASME Trans. Mechatronics* **23** 2952–62
- [25] Zhu Y, Wang X, Zheng J, Xiong H and Zhao Y 2020 Using GPS time-differenced carrier phase observations to calibrate LDV/INS integrated navigation systems *IEEE Sens. J.* **20** 405–14
- [26] Xiang Z, Wang Q, Huang R, Xi C, Nie X and Zhou J 2021 Position observation-based calibration method for an LDV/SINS integrated navigation system *Appl. Opt.* **60** 7869
- [27] Wang M, Cui J, Huang Y, Wu W and Du X 2021 Schmidt ST-EKF for autonomous land vehicle SINS/ODO/LDV integrated navigation *IEEE Trans. Instrum. Meas.* **70** 1–9
- [28] Xiang Z, Wang Q, Huang R, Xi C, Nie X and Zhou J 2022 In-motion initial alignment method for a laser Doppler velocimeter-aided strapdown inertial navigation system based on an adaptive unscented quaternion H-infinite filter *Meas. Sci. Technol.* **33** 035001
- [29] Xi C, Wang Q, Nie X, Huang R, Xiang Z, Zhou J and Jin S 2022 Online calibration technology for a one-dimensional laser Doppler velocimeter based on a strapdown inertial navigation system *Appl. Opt.* **61** 1229
- [30] Xiang Z, Wang Q, Huang R, Xi C, Nie X and Zhou J 2022 A fast robust in-motion alignment method for laser doppler velocimeter-aided strapdown inertial navigation system *IEEE Sens. J.* **22** 17254–65
- [31] Xu B, Wang L, Li S and Zhang J 2020 A novel calibration method of SINS/DVL integration navigation system based on quaternion *IEEE Sens. J.* **20** 1
- [32] Wang Q, Gao C, Zhou J, Wei G, Nie X and Long X 2018 Two-dimensional laser Doppler velocimeter and its integrated navigation with a strapdown inertial navigation system *Appl. Opt.* **57** 3334
- [33] Nie X and Zhou J 2020 Pitch independent vehicle-based laser Doppler velocimeter *Opt. Lasers Eng.* **131** 106072